

# Characterizing extinction debt following habitat fragmentation using neutral theory

Samuel E.D. Thompson<sup>1,2</sup>, Ryan A. Chisholm<sup>1</sup>, James Rosindell<sup>2</sup>

---

**Type of article:** Letter

**Running title:** Fragmentation and extinction debt

**Corresponding author:** Ryan A. Chisholm (ryan.chis@gmail.com)

**Keywords:** biodiversity, extinction debt, fragmentation, connectivity, habitat loss, spatially explicit, modelling, neutral theory

**Word Count:** 5000    **Abstract Word Count:** 150    **Reference Count:** 57

**Captions Word Count:** Fig. 1 (127), Fig. 2 (84), Fig. 3 (161), Fig. 4 (137), Fig. 5 (94), Fig. 6 (122)

**Author Contributions:** All authors designed the study. SEDT performed simulations and analyses.

All authors contributed to mathematical derivations. All authors wrote the paper.

**Data accessibility statement:** We confirm that, should the manuscript be accepted, all data supporting the results will be archived on Dryad with the DOI included at the end of the article and the code for analysis will be provided on bitbucket:

[https://bitbucket.org/thompsonsed/extinction\\_debt\\_eco\\_let](https://bitbucket.org/thompsonsed/extinction_debt_eco_let).

<sup>1</sup> Department of Biological Sciences, Faculty of Science, National University of Singapore, 14

Science Drive 4, 117543, Singapore

<sup>2</sup> Department of Life Sciences, Imperial College London, Silwood Park campus, Buckhurst Road,

Ascot, Berkshire SL5 7PY, UK

# 1 Abstract

2 Habitat loss leads to species extinctions, both immediately and over the long-term as “extinction  
3 debt” is repaid. The same quantity of habitat can be lost in different spatial patterns with varying  
4 habitat fragmentation. How this translates to species loss remains an open problem requiring an  
5 understanding of the interplay between community dynamics and habitat structure across  
6 temporal and spatial scales. Here we develop formulas that characterize extinction debt in a  
7 spatial neutral model after habitat loss and fragmentation. Central to our formulas are two new  
8 metrics, which depend on properties of the taxa and landscape: “effective area”, measuring the  
9 remaining number of individuals; and “effective connectivity”, measuring individuals’ ability to  
10 disperse through fragmented habitat. This formalizes the conventional wisdom that habitat area  
11 and habitat connectivity are the two critical requirements for long-term preservation of  
12 biodiversity. Our approach suggests that mechanistic fragmentation metrics help resolve debates  
13 about fragmentation and species loss.

## 14 Introduction

15 Habitat loss drives extinction (Millenium Ecosystem Assessment 2005; Rybicki & Hanski 2013). If  
16 all remaining individuals of a species immediately perish during habitat loss, then that species  
17 becomes extinct. Surviving species may still be driven to extinction after the habitat loss via  
18 ongoing processes. These delayed extinctions constitute an “extinction debt” resulting from past  
19 landscape changes (Tilman *et al.* 1994). Forecasting extinction debt is challenging and requires  
20 understanding how many species exist immediately after habitat loss and how many will persist  
21 at equilibrium in the long-term (Hanski & Ovaskainen 2002; Hanski 2011).

22 Habitat loss is often accompanied by habitat fragmentation: the process of dividing a large  
23 contiguous region of habitat into smaller, spatially disjunct remnants. In a fragmented landscape,  
24 edge effects, patch size and isolation between patches—in addition to habitat area—all influence  
25 species richness (Didham & Lawton 1999; Wilson *et al.* 2016) and thus have a bearing on  
26 extinction debt. Furthermore, different taxa can exhibit different responses to habitat loss, even  
27 within the same area (Carrara *et al.* 2015). These differences are dependent on both local and  
28 regional habitat configuration (Tischendorf & Fahrig 2000).

29 While it is uncontroversial that species richness decreases with loss of total habitat area, the  
30 relationship between species richness and habitat fragmentation for a specific level of habitat  
31 area (habitat fragmentation *per se*) remains the subject of fervent debate. Some authors claim  
32 the relationship is generally positive (Fahrig 2017, 2019; Fahrig *et al.* 2019; May *et al.* 2019);  
33 others claim it is negative (Wilson *et al.* 2016; Thompson *et al.* 2017; Fletcher *et al.* 2018). Part of  
34 the problem is that observational studies informing the debate are relatively few, and

35 experimental studies are even fewer (see Fahrig 2017 for a review). Even modelling studies on  
36 fragmentation and biodiversity are restricted in scale, because the spatially explicit models  
37 needed are computational expensive.

38 One way to avoid the computational cost of simulation modelling is to develop formulas that  
39 relate species richness to fragmentation. Standard formulas for estimating species loss from  
40 habitat loss ignore fragmentation entirely. A typical method is to take a species–area relationship  
41 (SAR) formula, such as the power law, and estimate species loss as the difference between the  
42 estimated species richness of the original area and that of the smaller area remaining after  
43 habitat loss (Brown 1984; Durrett & Levin 1996; Thomas *et al.* 2004; Foster *et al.* 2013). In  
44 addition to their failure to account for fragmentation, another limitation of standard SAR  
45 methods is that they ignore the temporal component of species loss, i.e., they are insensitive to  
46 the differences between species richness in the short-term compared with the long-term  
47 following habitat loss. Attempts to salvage the power-law SAR by parameterizing it for different  
48 temporal scales (Rosenzweig 1995; Rosenzweig & Ziv 1999) or different degrees of fragmentation  
49 (Hanski *et al.* 2013; Haddad *et al.* 2015) still do not avoid the basic limitation that the power-law  
50 is a phenomenological model. Such models cannot yield ecological insights or accurate  
51 predictions outside the range of the data used for parameterization. This is particularly  
52 problematic when applied to extinction debt as there is a paucity of long-term data. New  
53 mechanistic formulas relating the effects of fragmentation to species loss and extinction debt are  
54 sorely needed.

55

56 One fundamental issue, which we believe has confounded both the fragmentation–diversity  
57 debate and efforts to develop species–area–fragmentation formulas, is the lack of clarity about  
58 how to measure fragmentation (Ewers & Didham 2007; Lindenmayer & Fischer 2007). A host of  
59 metrics exist for characterizing features of spatially intricate habitat structure (Wang *et al.* 2014;  
60 Turner & Gardner 2015). No single metric has prevailed as a way to define or quantify  
61 fragmentation and it is not clear which existing metrics are most relevant. An alternative  
62 approach is to avoid fragmentation metrics by simulating a mechanistic community model on a  
63 spatially explicit replica of the fragmented landscape (Hanski *et al.* 2013; Rybicki & Hanski 2013).  
64 However, the simulation approach is computationally expensive and only narrowly applicable to  
65 the simulated scenario. This again points to the need for formulas, but more specifically, for  
66 formulas that quantify fragmentation – through an appropriate fragmentation metric – in a way  
67 that is relevant to biodiversity.

68 What kinds of models may be suitable for deriving species–area–fragmentation formulas? Ideally,  
69 the models should be mechanistic and parsimonious, to facilitate generality and tractability. One  
70 such class of models is individual-based neutral models (Hubbell 2001), which assume that an  
71 individual’s species identity does not influence its chances of survival or reproduction. Despite  
72 their assumptions, neutral models can reproduce numerous patterns of biodiversity (Volkov *et al.*  
73 2003, 2007; Alonso *et al.* 2006) and non-spatial versions have been applied to predict species loss  
74 (Gilbert *et al.* 2006; Hubbell *et al.* 2008; Halley & Iwasa 2011; Halley *et al.* 2014). More germane  
75 to the inherently spatial problem of extinction debt are spatially explicit neutral models (Chave &  
76 Leigh 2002; Chave & Norden 2007; Rosindell & Cornell 2007, 2009), which are less  
77 comprehensively studied. While most studies of spatially explicit neutral models assume 100%

78 habitat cover, a few have considered more general landscapes with habitat configurations that  
79 could represent real habitat-loss scenarios (Pereira *et al.* 2012; Campos *et al.* 2013). Analytical  
80 formulas for species richness in spatially explicit neutral models have recently been derived for  
81 the special case where habitat is contiguous and has not been destroyed or fragmented (O’Dwyer  
82 & Cornell 2018). These formulas have been extended to predict immediate species loss following  
83 special kinds of fragmented habitat loss (Chisholm *et al.* 2018), but the problem of long-term  
84 species losses and extinction debt in such models has yet to be tackled.

85 Here we help bring clarity to the fragmentation–diversity debate by developing what are, to our  
86 knowledge, the first analytical solutions for quantifying long-term species loss and extinction debt  
87 under fragmentation scenarios in a mechanistic model. We use the spatially explicit neutral  
88 model, but highlight how our approach can be generalized to environments with multiple niches.  
89 Our formulas predict extinction debt based on the change in a habitat’s “effective area”, which  
90 captures the number of individuals supported in the remaining habitat, and “effective  
91 connectivity”, which captures ease of movement through the landscape from the perspective of  
92 the taxa being studied and their dispersal ability. These two novel metrics give a rigorous  
93 analytical grounding to the long-held view of conservation biologists that habitat area and habitat  
94 connectivity are what drive long-term biodiversity preservation.

## 95 Methods

96 Our methods comprised three steps. First, we derived new analytical formulas for estimating  
97 long-term species loss in fragmented landscapes under a mechanistic neutral model. Second, we  
98 verified our formulas by comparing their predictions to individual-based neutral simulations on

99 fragmented landscapes including real landscapes from satellite data and synthetic landscapes  
100 generated algorithmically. Third, we used the formulas to get new conceptual insights about the  
101 general relationship of extinction debt to landscape and taxa.

## 102 Spatially explicit neutral models

103 Our model generates spatially explicit neutral communities in a manner broadly similar to the  
104 simulations used in Rosindell & Cornell (2007). Every time step, an individual is killed and the  
105 replacement is chosen from the propagules landing at the newly vacated cell. Each individual  
106 rains propagules onto the surrounding landscape in a radially symmetric pattern according to a  
107 dispersal kernel. With some small probability  $\nu$ , the individual mutates into a new species  
108 (speciation). Eventually, a dynamic equilibrium between speciation, immigration and extinction is  
109 reached at the landscape scale. Predictions from these models are robust to changes in the  
110 dispersal kernel (Rosindell & Cornell 2007, 2009) and coincide with those of the non-spatial model  
111 at large scales (Rosindell & Cornell 2013). Coalescence methods enable efficient simulations on a  
112 subset of individuals within effectively infinite landscapes (Rosindell *et al.* 2008). They work by  
113 progressing backwards in time, tracking only the ancestors to present-day individuals of interest.  
114 We tracked the species richness within a single tile (a “focal region”) of an infinite landscape  
115 constructed by tiling a given landscape structure. Simulations were implemented in C++ and  
116 Python using the pycoalescence package (available on bitbucket:  
117 <https://bitbucket.org/thompsonsed/pycoalescence>).

118

119 Analytical approach

120 We sought to derive analytical formulas for long-term species loss following habitat loss in a  
121 spatially explicit neutral model. In contrast to Chisholm *et al.* (2018), who studied a similar system  
122 and focused on species loss immediately following habitat clearing, we focused on the long-term  
123 outcome. We used a method common in physics whereby a complex system can be re-written in  
124 terms of a reduced number of parameters. The approach involves determining combinations of  
125 parameters that are codependent, meaning the full solution for the system can ultimately be  
126 reduced to simpler, analytically tractable cases (as in Rosindell & Cornell 2007; Chisholm *et al.*  
127 2018). Such approaches are typically developed by examination of simulation results, heuristic  
128 arguments and inspired guesswork; they are later verified by extensive simulation.

129 In the standard spatially explicit neutral model using gaussian dispersal and point mutation,  
130 species richness in a defined region of a contiguous, infinite landscape reaches a dynamic  
131 equilibrium between speciation, immigration, and extinction and can be described by a two-  
132 parameter function known as the “Preston function”  $\Psi$  (Chisholm *et al.* 2018; O’Dwyer & Cornell  
133 2018; Appendix 1). Following a tradition of naming special functions in mathematics, the Preston  
134 function was named (Chisholm *et al.* 2018) to highlight its importance and to abstract away the  
135 complicated analytical solution (O’Dwyer & Cornell 2018). Specifically, the species richness of a  
136 disc-shaped focal area, set within an infinite contiguous neutral landscape, can be approximated  
137 as

$$S_{\text{contig}}(A_e, \nu, \sigma^2) \sim \sigma^2 \Psi\left(\frac{A_e}{\sigma^2}, \nu\right)$$

138 (1)



139 where  $\nu$  is the point speciation rate,  $\sigma^2$  is a measure of dispersal ability (the variance of a  
140 bivariate normal dispersal kernel) and  $A_e$  is the number of individual organisms in the focal area  
141 (O’Dwyer & Cornell 2018). Chisholm *et al.* (2018) extended this result to produce equations giving  
142 upper and lower bounds on species loss immediately after habitat loss. We calculated extinction  
143 debt in the same model by deriving the long-term species richness following habitat loss and  
144 taking the difference between this and the species richness immediately after habitat loss. To  
145 distinguish our results from previously derived formulas for  $S$  the species richness immediately  
146 following habitat loss, we developed a hat notation  $\hat{S}$  to indicate long-term species richness at  
147 equilibrium following habitat loss. Whilst both  $S$  and  $\hat{S}$  are expressed in terms of Preston  
148 functions, their mathematical forms and biological meanings are very different. Estimating  $S$  is a  
149 relatively simple spatial sampling problem; estimating long-term species richness  $\hat{S}$  involves  
150 community dynamics on the fragmented landscape.

151

## 152 Landscape generation

153 In order to verify our analytical results, we performed simulations on a wide variety of “synthetic”  
154 and “real” landscapes. Two parameters defined the landscapes:  $h$ , the percentage of habitat  
155 cover after loss; and  $A_{\max}$ , the maximum possible “effective area” in the landscape with 100%  
156 habitat cover, where we define effective area as the number of individual organisms present in a  
157 focal landscape. The effective area after habitat loss is given by  $A_e = h \cdot A_{\max}$ . We used  $A_{\max}$   
158 values of  $50^2$ ,  $500^2$  and  $5000^2$ , and  $h$  values of 10, 20 or 40% yielding nine values of  $A_e$ . All

159 habitat pixels within our landscapes had equal value to organisms, and all non-habitat pixels had  
160 zero value.

161 Our synthetic landscapes comprised two types: “random” (Fig. 1a) and “clustered” (Fig. 1b).

162 Random landscapes were produced from a landscape with 100% habitat by randomly removing  
163 pixels until the desired habitat cover was achieved. Ten random landscapes were generated for  
164 each value of landscape size  $A_{\max}$  and percent cover  $h$ , giving a total of 90 maps. Clustered  
165 landscapes consisted of evenly spaced disc-shaped clusters of habitat and had one additional  
166 parameter: the number of fragments  $n$ . Clustered landscapes were produced for  $n = 2^i$  where  
167  $i$  ranges from 0 (a single large fragment) to  $\log_2 A_e$  (every individual an isolated patch).

168 Our real landscapes (Fig. 1c) came from satellite maps of South American forest cover (Hansen *et*  
169 *al.* 2013). Our models on these maps are not intended to represent Amazon tree community  
170 dynamics specifically; the maps provide a selection of realistic landscape patterns for testing our  
171 formulas. For each value of  $h$ , regions with habitat cover within 1% of  $h$  were identified and pixels  
172 added to or removed from habitat boundaries to produce maps that had exactly the desired  
173 habitat cover (but still closely resembled real landscapes). For  $A_{\max} = 5000^2$  there were  
174 insufficient regions with habitat areas within 1% of the target parameter values so instead one  
175 hundred randomly chosen real maps each of size  $A_{\max} = 500^2$  were tiled to create these  
176 landscapes.

177 Empirical example

178 To provide examples of how our methods can be applied, we also estimated actual extinction  
179 debt for tropical trees in five specific regions of the Amazon. The forest cover satellite maps from

180 Hansen *et al.* (2013) provided the spatial arrangement of trees within each region. The five sites  
 181 experienced significant deforestation in the last twenty years and were chosen with relatively  
 182 similar patterns of fragmentation across a large area surrounding the focal landscape. The model  
 183 parameters were taken from the tropical forest literature (Condit *et al.* 2012): a density of 0.0512  
 184 individual adult trees per  $\text{m}^2$ , a dispersal parameter of  $\sigma = 8.5$  (approximately 40.2 m) and a  
 185 speciation rate of  $\nu = 6 \times 10^{-6}$ .

## 186 Results

### 187 Analytical solutions for long-term species richness in simple 188 landscapes

189 Finding a general analytical solution from our neutral models for long-term (equilibrium) species  
 190 richness,  $\hat{S}$ , of the focal region within an infinite landscape  $\mathbf{L}$  requires understanding which  
 191 features of  $\mathbf{L}$  are most important for ecological processes. In the special case of a contiguous  
 192 landscape  $\mathbf{L}_{\text{contig}}$  with 100% habitat cover, no habitat has been lost and  $A_e = A_{\text{max}}$ . The long-  
 193 term equilibrium species richness is therefore equal to the original species richness:

$$\hat{S}(\mathbf{L}_{\text{contig}}, \nu, \sigma^2) = \hat{S}_{\text{contig}}(A_{\text{max}}, \nu, \sigma^2) = S_{\text{contig}}(A_{\text{max}}, \nu, \sigma^2) \sim \sigma^2 \Psi\left(\frac{A_{\text{max}}}{\sigma^2}, \nu\right)$$

194 (2)

195 Randomly fragmented landscapes represent another special case: here habitat cells are uniformly  
 196 distributed in space, just like the contiguous case, only now they are randomly mixed with non-  
 197 habitat cells that cannot be occupied. The average distance between adjacent habitat cells is

198  $\sqrt{\frac{A_{\max}}{A_e}}$  cell widths instead of one cell width in the contiguous case. A heuristic solution to long-  
 199 term species richness can be obtained as follows: if we imagine compressing the spaces between  
 200 habitat cells by  $\sqrt{\frac{A_e}{A_{\max}}}$  and reducing the dispersal distance  $\sigma$  by the same factor, the community  
 201 dynamics of the system would be unchanged, but now the habitat cells would be contiguous in  
 202 space. For the randomly fragmented landscape  $\mathbf{L}_{\text{random}}$ , the equilibrium long-term diversity  
 203  $\hat{S}_{\text{random}}$  can thus be calculated in terms of Preston functions by substituting  $\sqrt{\frac{A_e}{A_{\max}}}\sigma$  for  $\sigma$  in Eq.  
 204 (2):

$$205 \hat{S}(\mathbf{L}_{\text{random}}, \nu, \sigma^2) = \hat{S}_{\text{random}}(A_{\max}, A_e, \nu, \sigma^2) = \hat{S}_{\text{contig}}\left(A_e, \nu, \frac{A_e}{A_{\max}}\sigma^2\right) \sim \frac{A_e}{A_{\max}}\sigma^2\Psi\left(\frac{A_{\max}}{\sigma^2}, \nu\right)$$

206 (3)

207 We verified this result numerically (Appendix 3); the mean percentage error (MPE) was less than  
 208 4% and can be attributed to the error inherent to the current methods for evaluating the Preston  
 209 function itself (O'Dwyer & Cornell 2018).

## 210 Analytical solutions for complex landscapes: incorporating 211 effective connectivity

212 We have thus far considered the idealized contiguous and random habitat patterns, but most  
 213 landscapes exhibit some intermediate fragmented spatial structure (Fig. 1) that is described by  
 214 neither of the extreme cases corresponding to Eqs. (2) and (3) (Appendix 3). There is no single  
 215 metric that entirely captures fragmentation, or even an agreement among ecologists on the strict

216 definition of fragmentation. Our strategy here is to side-step this definitional issue and instead  
217 introduce metrics of the landscape that are mechanistically important for species diversity.

218 We conjectured that a fruitful approach for developing fragmentation metrics relevant to  
219 biodiversity would be to consider fragmentation from the perspective of a dispersing organism.  
220 Due to the shape of a fragmented habitat, the effective dispersal—the actual movement across a  
221 fragmented landscape—may differ considerably from the intrinsic dispersal—the expected  
222 movement of the same taxa on a contiguous landscape. We developed an “effective dispersal”  
223 metric  $\sigma_e$ , which is calculated algorithmically by sequentially applying  $n$  dispersal events and  
224 recording the total distance between the overall start and end points. By repeating the process  
225 starting from different habitat cells, we generated the mean distance  $\mu_n$  travelled over  $n$   
226 generations for the landscape. Relating this distance back to a per-generation equivalent gives  
227 our effective dispersal parameter  $\sigma_e^2 \approx \mu_n^2 \cdot \frac{2}{n\pi}$  (Appendix 2). For  $n > 1$  this metric adds weight to  
228 the connectivity in critical regions through which many lineages pass over longer time scales. In  
229 our calculations we used  $n = 1/\nu$ , the expected species’ lifetime. This means that the landscape  
230 structure surrounding the focal area has influence growing weaker with distance, but decaying to  
231 zero only on passing the range boundary of an average species present in the focal region. In  
232 most cases the estimate of  $\sigma_e$  converged for much lower values of  $n \approx 1000$ .

233 We then defined another novel metric that we call “effective connectivity”  $c_e$ , which combines  
234 the proportional habitat coverage with effective dispersal. This makes our metric a function of  
235 both habitat configuration and properties of the taxa of interest, distinguishing itself from other  
236 landscape metrics that statically capture habitat configuration only. We define effective  
237 connectivity for a single cell in terms of its squared value, which is the squared mean distance

238 travelled per generation for lineages starting from that cell, if the cell is habitat, or zero, if the cell  
239 is not habitat (i.e., it contains no individuals). Averaging over all cells gives the effective  
240 connectivity of the whole landscape:

$$c_e^2 = h \cdot \sigma_e^2$$

241 (4)

242 where  $h$  is the proportion of habitat cover ( $h = \frac{A_e}{A_{\max}}$ ) and  $\sigma_e$  is the effective dispersal, as defined  
243 above.

244 We found that the calculation for effective connectivity can be performed with reasonable  
245 accuracy in equivalent computational time to other landscape metrics such as average patch size  
246 and edge-to-area ratio (see Hesselbarth *et al.* 2019). We used heuristic arguments involving the  
247 effective connectivity metric to develop the following ansatz for equilibrium species richness in a  
248 neutral model on a fragmented landscape:

$$\hat{S}(\mathbf{L}, \nu, \sigma^2) = \hat{S}_{\text{contig}}(A_e, \nu, c_e^2) \sim c_e^2 \Psi\left(\frac{A_e}{c_e^2}, \nu\right)$$

249 (5)

250 The motivation for this formula comes from the intuition that a generic landscape gives the same  
251 long-term result as a contiguous landscape with augmented dispersal to account for the change in  
252 connectivity. As expected, Eq. (5) reduces to Eq. (2) in the special case that the landscape is  
253 contiguous and to Eq. (3) in the special case that the landscape is randomly fragmented.

## 254 Verifying analytical results

255 We confirmed by simulation that our new general solution for long-term species richness (Eq. (5))  
256 accurately matches simulated species richness values (Appendix 3 Fig. S3). The analytical values  
257 have under 10% MPE across landscape types (8.1%, 9.1% and 4.2% for real, clustered and random  
258 landscapes, respectively) when compared against simulated values. The power of our approach  
259 can be seen by rearranging Eq. (5) to give

$$\frac{1}{c_e^2} \hat{S}(\mathbf{L}, \nu, \sigma^2) \sim \Psi\left(\frac{A_e}{c_e^2}, \nu\right)$$

260 (6)

261 Eq. (6) predicts that plotting species richness and effective area both rescaled by effective  
262 connectivity (i.e.,  $\frac{\hat{S}}{c_e^2}$  versus  $\frac{A_e}{c_e^2}$ ) should cause the SARs for all fragmented landscapes to collapse on  
263 to one curve. We verified this was true for all our simulated data (Fig. 2b) despite the huge  
264 variability displayed by the unscaled SARs (Fig. 2a). This scaling collapse verifies that we can  
265 estimate species loss by calculating just two parameters from our fragmented landscape  
266 (effective area  $A_e$  and effective connectivity  $c_e$ ) and plugging the numbers into our Eq. (5). Doing  
267 so produced noteworthy errors only for a small number of special cases corresponding to  
268 clustered landscapes with extremely low effective connectivity due to the presence of highly  
269 isolated habitat ‘islands’. On such landscapes, the simulated long-term richness was relatively  
270 high because of endemism on the ‘islands’, but the scaling used to produce Eq. (5) cannot account  
271 for such endemics and thus underestimates species richness (see Appendix 3).

## 272 Extinction debt

273 We applied our new analytical methods to the problem of estimating extinction debt in  
274 fragmented landscapes. The upper and lower bounds on species richness immediately after  
275 habitat loss, for given values of the fragmentation-independent parameters ( $A_e$ ,  $A_{\max}$  and  $\sigma$ ), are  
276 given by formulas in Chisholm *et al.* (2018). Our new results provide the corresponding estimates  
277 of long-term loss. We calculated upper and lower bounds on  $\sigma_e$  for each  $A_{\max}$  from the minimum  
278 and maximum values across all the real and synthetic landscapes; this in turn gives bounds on  
279 effective connectivity  $c_e$  and ultimately on  $\hat{S}$  (via Eq. (4)), representing the best- and worst-case  
280 scenarios for long-term species richness on fragmented landscapes (Appendix 4). Corresponding  
281 estimates of extinction debt are given in absolute terms as  $S - \hat{S}$  or in relative terms as  $(S - \hat{S})/$   
282  $S_0$ , where  $S_0$  is the species richness of the original landscape.

283 Across a range of spatial scales ( $A_{\max}$ ), levels of habitat cover ( $\frac{A_e}{A_{\max}}$ ) and intrinsic dispersal  
284 parameters ( $\sigma$ ), immediate species loss was consistently substantial, but usually represented less  
285 than 50% of species richness (Fig. 3). By contrast, when extinction debt was accounted for, total  
286 long-term losses were usually over 50% and in many cases close to 100%. The qualitative  
287 relationship of immediate and long-term loss to spatial scale was consistent across parameter  
288 sets (Appendix 4): extinction debt (in relative terms) was generally maximal at intermediate scales  
289 but remained sensitive to the spatial structure of each habitat.

290 Among the suite of landscapes in our testbed, the real landscapes from satellite data are most  
291 relevant for empirical problems. Our simulation-based estimates of long-term species loss on  
292 these real landscapes fell within the theoretical bounds from our formulas, as expected, but



293 exhibited a much narrower range of values than those from our synthetic landscapes. For small  
 294 real landscapes, the percentage long-term species loss was approximately equal to the  
 295 percentage of habitat loss (Fig. 4). At intermediate spatial scales the percentage long-term species  
 296 loss was greatest: for example, for the parameter values in Fig. 4, long-term species loss on real  
 297 landscapes was 90–95% at intermediate spatial scales when 80% of habitat was lost. At very large  
 298 scales, we found that the structure of real landscapes tended to impede dispersal, leading to low  
 299  $c_e$  values and long-term species richness values close to the theoretical lower bound (Fig. 4).

300 In an example application of our methods, estimating tree species losses in the Amazon (Fig. 6)  
 301 the predicted species richness was consistently closer to the theoretical lower bound. Overall, the  
 302 percentage of species remaining as a function of spatial scale follows a U-shaped curve on real  
 303 landscapes (Fig. 4), and accordingly the total percentage of species lost (extinction debt and  
 304 immediate loss together) follows a hump-shaped curve. In Fig. 5, we summarize graphically the  
 305 expected percentage of species remaining for a range of levels of habitat loss and connectivity  
 306 and across a range of spatial scales.

307 We found that the most connected scenario in our model, and the best-case scenario for long-  
 308 term species richness (lowest species loss), is when habitat loss is random. We can quantify this  
 309 best-case scenario by taking the long-term species richness from a randomly fragmented  
 310 landscape divided by the original species richness in a contiguous landscape:

$$\frac{\hat{S}_{random}(A_{max}, A_e, \nu, \sigma^2)}{S_{contig}(A_{max}, \nu, \sigma^2)} = \frac{\frac{A_e}{A_{max}} \sigma^2 \Psi\left(\frac{A_{max}}{\sigma^2}, \nu\right)}{\sigma^2 \Psi\left(\frac{A_{max}}{\sigma^2}, \nu\right)} = \frac{A_e}{A_{max}}$$

311 (6)

312 Therefore, the best-case proportion of species remaining in the long-term after habitat loss is  
313 equal to the proportion of habitat remaining  $h = \frac{A_e}{A_{\max}}$  (Fig. 6). This result also generalizes to the  
314 case where the landscape consists of multiple habitat types each providing an independent niche  
315 for species to occupy, assuming that within each niche species dynamics are neutral (Appendix 6).  
316 Even this best-case long-term scenario is substantially worse than immediate loss scenarios,  
317 where the number of species initially remaining is always higher than  $\frac{A_e}{A_{\max}}$  (Fig. 6b). The  
318 importance of accurately accounting for extinction debt is underscored by a comparison with the  
319 traditional power-law SAR approach, which in a scenario of 20% habitat remaining predicts the  
320 62–85% of species remaining (Appendix 1), a substantial overestimate compared to our results  
321 (Fig. 6a).

## 322 Discussion

323 Habitat loss is a ubiquitous feature of modern landscapes, yet we still lack a fundamental  
324 understanding of how it affects biodiversity both in the short-term and in the long-term after  
325 repayment of extinction debt. The effects of fragmentation on biodiversity in particular are hotly  
326 debated (Fahrig 2017; Fletcher *et al.* 2018) fueled partly, in our view, by lack of clarity around  
327 how to quantify fragmentation. The true response of biodiversity to fragmentation likely varies  
328 across spatial and temporal scales and is affected by properties of both species and landscapes  
329 (Lindenmayer *et al.* 2000, 2015; Evans *et al.* 2017). Here we have focused on the knowledge gap  
330 surrounding habitat loss, habitat fragmentation and extinction debt by developing new analytical  
331 treatments of a spatially explicit neutral model (Eq. (5)). Below we focus first on our technical  
332 results and then on the implications for the fragmentation debate more broadly.

333 Our neutral models account for fragmentation through new parameters, which measure  
334 landscapes through the lens of the taxa being studied. In particular, effective area  $A_e$  and  
335 effective connectivity  $c_e$  quantify concepts that have long been central to thinking in  
336 conservation. Our effective area parameter is the number of individual organisms remaining in  
337 the fragmented landscape and thus incorporates habitat quality and individual density for the  
338 taxa of interest. Our effective connectivity parameter integrates further aspects of habitat  
339 structure and dispersal mechanisms into a single value capturing broad restrictions to movement  
340 in the landscape for the taxa of interest. The broader lesson here is that any biologically  
341 meaningful metric of fragmentation must take a species-eye view of the world, rather than being  
342 based on human perceptions of what “fragmented” looks like.

343 What degree of species loss can be expected in the long term in a neutral model? Even in our  
344 best-case scenario, long-term species loss is substantial (Fig. 3), with the same proportion of  
345 species lost as the proportion of habitat lost. Worryingly, all our examples based on real  
346 fragmentation maps (Fig. 4, Fig. 6) are even more severe and closer to the worst-case scenario.  
347 This suggests that realistic landscape patterns exhibit considerable structural impediments to  
348 connectivity. In the real world, where competitive exclusion and environmental stochasticity  
349 accelerate change beyond the pace of a neutral model (Kalyuzhny *et al.* 2015; Danino *et al.* 2016),  
350 and where dispersal across the matrix may increase mortality, the loss of diversity could be  
351 greater still.

352 One prediction of our model is that the best-case scenario for long-term species richness, under a  
353 fixed total area of habitat loss, is a randomly cleared landscape corresponding to the highest  
354 connectivity between habitat cells. This prediction should be interpreted cautiously because our  
355 model ignores edge effects (see Appendix 5), which constitute a complex variety of ecological  
356 responses, with some positive but mostly negative effects on diversity. Along edges, sensitive  
357 species can be driven to extinction by processes including altered microclimate or increased  
358 accessibility to poachers (Ewers & Didham 2006; Evans *et al.* 2017). These extinctions can also be  
359 masked along edges by increased local habitat diversity. Our model could be extended to include  
360 edge effects by appropriately adjusting effective area to penalize edges.

361 Our analysis has exposed one general obstacle to a rigorous conceptual foundation of “extinction  
362 debt”. A practical definition of extinction debt in conservation biology would be based on a  
363 timescale that is long enough for a new equilibrium to be reached after fragmentation, but short  
364 enough that no significant speciation occurs. But when the ecological and evolutionary timescales

365 overlap (e.g., in Fig. 1, which indicates roughly 50,000 yr), it becomes impossible to satisfy both of  
366 these requirements simultaneously, because there is no true equilibrium on the ecological  
367 timescale. This suggests that defining extinction debt means specifying a timescale of interest,  
368 and that this choice will inevitably be somewhat arbitrary: the timescale must be long enough for  
369 most extinctions to occur, but short enough that speciation is still largely irrelevant.

370 Moving beyond the purview of conservation biology, we see that on very long (geological) time  
371 scales, fragmentation can actually increase diversity by promoting speciation (Fig. 1). It may seem  
372 paradoxical that anthropogenic habitat fragmentation is generally thought to be bad for  
373 biodiversity whilst geological habitat fragmentation is perceived to increase diversity due to  
374 speciation and the origin of endemics in isolated habitat patches such as the islands on  
375 archipelagos. The phenomenon is of great interest in biogeography: repeated bouts of  
376 fragmentation and speciation over geological time is one hypothesis proposed to explain the high  
377 diversity and endemism of ecosystems ranging from the Amazon to the South African fynbos  
378 (Allsopp et al. 2014). It is pleasing that a single unified model provides explanations for why  
379 fragmentation can destroy biodiversity on short term time scales, yet sometimes foster  
380 biodiversity on geological timescale (see Appendix 4). Also, these results highlight the conundrum  
381 that reconnecting historically fragmented landscapes can have a negative impact on biodiversity,  
382 a topic that we leave for future work.

383 Returning to the ongoing fragmentation debate (Fahrig 2017, 2019; Fletcher *et al.* 2018; Fahrig *et*  
384 *al.* 2019; Miller-Rushing *et al.* 2019), we ascribe the current impasse partly to differences in the  
385 unstated assumptions made by the opposing sides, which in turn is due to a reliance on mainly on  
386 verbal arguments inspired by intuition and limited empirical evidence. If even in a neutral model,

387 the answer to the fragmentation question is non-trivial and context-dependent, surely it must be  
388 so in reality as well. Therefore, we encourage participants in the fragmentation debate to take  
389 pains to make explicit their assumptions about spatial scales, temporal scales, taxonomic scope,  
390 and the definition of fragmentation itself. More quantitative mechanistic modelling could help in  
391 this regard.

392 Beyond these general recommendations, we highlight three key messages for the fragmentation  
393 debate. First, the response of species to fragmentation depends not just on the arrangement and  
394 amount of habitat loss, but on ecological properties of the species themselves, including dispersal  
395 ability. Second, the long-term species loss following habitat loss can be drastically different to the  
396 immediate species loss. Finally, quantifying fragmentation in a mechanistic way – here using our  
397 effective connectivity and effective area metrics – is critical to properly understanding its impact.

398 We have presented a new analysis of a mechanistic model that allows us to hone our intuitions  
399 for how the process of fragmentation and habitat loss affects diversity over different spatial and  
400 temporal scales. In characterizing the response of biodiversity to fragmentation, we show that  
401 doing so accurately requires an appropriate metric of fragmentation that specifically considers  
402 species' responses to fragmentation (effective connectivity). We hope that this will be used as the  
403 foundation for more sophisticated models forecasting diversity loss.

## 404 Acknowledgements

405 We thank the editor and three anonymous reviewers for helpful feedback on earlier versions of  
406 this manuscript. We also thank Nadiah Kristensen for comments on the manuscript and Tak Fung  
407 and Rogier Hintzen for many helpful discussions. S.E.D.T was supported by the Joint Imperial-NUS

408 PhD Scholarship. R.A.C was supported by grants from the James. S. McDonnell Foundation  
409 (#220020470) and the Singapore Ministry of Education (WBS R-154-000-A12-114). J.R. was  
410 funded by fellowships from the Natural Environment Research Council (NERC) (NE/I021179,  
411 NE/L011611/1). This study is a contribution to Imperial College’s Grand Challenges in Ecosystems  
412 and the Environment initiative. All simulations were run on high throughput compute systems at  
413 Imperial College London.

## 414 References

- 415 Allsopp, N., Colville, J.F. & Verboom, G.A. (2014). Fynbos: ecology, evolution and conservation of a  
416 megadiverse region. *Fynbos Ecol. Evol. Conserv. a megadiverse Reg.*, 382.
- 417 Alonso, D., Etienne, R.S. & McKane, A.J. (2006). The merits of neutral theory. *Trends Ecol. Evol.*,  
418 21, 451–457.
- 419 Brown, J.H. (1984). On the Relationship between Abundance and Distribution of Species. *Am.*  
420 *Nat.*, 124, 255–279.
- 421 Campos, P.R.A., Rosas, A., de Oliveira, V.M. & Gomes, M.A.F. (2013). Effect of Landscape  
422 Structure on Species Diversity. *PLoS One*, 8, e66495.
- 423 Carrara, E., Arroyo-Rodríguez, V., Vega-Rivera, J.H., Schondube, J.E., de Freitas, S.M. & Fahrig, L.  
424 (2015). Impact of landscape composition and configuration on forest specialist and generalist  
425 bird species in the fragmented Lacandona rainforest, Mexico. *Biol. Conserv.*, 184, 117–126.
- 426 Chave, J. & Leigh, E.G. (2002). A Spatially Explicit Neutral Model of b-Diversity in Tropical Forests.  
427 *Theor. Popul. Biol.*, 62, 153–168.

- 428 Chave, J. & Norden, N. (2007). Changes of species diversity in a simulated fragmented neutral  
429 landscape. *Ecol. Modell.*, 207, 3–10.
- 430 Chisholm, R.A., Lim, F., Yeoh, Y.S., Seah, W.W., Condit, R. & Rosindell, J. (2018). Species–area  
431 relationships and biodiversity loss in fragmented landscapes. *Ecol. Lett.*, 21, 804–813.
- 432 Condit, R., Lao, S., Pérez, R., Dolins, S.B., Foster, R.B. & Hubbell, S.P. (2012). Barro Colorado Forest  
433 Census Plot Data, 2012 Version. *Cent. Trop. For. Sci. Databases*.
- 434 Condit, R., Pitman, N., Leigh, E.G., Chave, J., Terborgh, J., Foster, R.B., *et al.* (2002). Beta-diversity  
435 in tropical forest trees. *Science (80-. )*, 295, 666–669.
- 436 Danino, M., Shnerb, N.M., Azaele, S., Kunin, W.E. & Kessler, D.A. (2016). The effect of  
437 environmental stochasticity on species richness in neutral communities. *J. Theor. Biol.*, 409,  
438 155–164.
- 439 Didham, R.K. & Lawton, J.H. (1999). Edge Structure Determines the Magnitude of Changes in  
440 Microclimate and Vegetation Structure in Tropical Forest Fragments. *Biotropica*, 31, 17.
- 441 Durrett, R. & Levin, S. (1996). Spatial models for species-area curves. *J. Theor. Biol.*, 179, 119–127.
- 442 Evans, M.J., Banks, S.C., Driscoll, D.A., Hicks, A.J., Melbourne, B.A. & Davies, K.F. (2017). Short-and  
443 long-term effects of habitat fragmentation differ but are predicted by response to the  
444 matrix. *Ecology*, 98, 807–819.
- 445 Ewers, R.M. & Didham, R.K. (2006). Confounding factors in the detection of species responses to  
446 habitat fragmentation. *Biol. Rev. Camb. Philos. Soc.*, 81, 117–142.



- 447 Ewers, R.M. & Didham, R.K. (2007). Habitat fragmentation: panchreston or paradigm? *Trends*  
448 *Ecol. Evol.*, 22, 511.
- 449 Fahrig, L. (2017). Ecological Responses to Habitat Fragmentation Per Se. *Annu. Rev. Ecol. Evol.*  
450 *Syst.*, 48, annurev-ecolsys-110316-022612.
- 451 Fahrig, L. (2019). Habitat fragmentation: A long and tangled tale. *Glob. Ecol. Biogeogr.*, 28, 33–41.
- 452 Fahrig, L., Arroyo-Rodríguez, V., Bennett, J.R., Boucher-Lalonde, V., Cazetta, E., Currie, D.J., *et al.*  
453 (2019). Is habitat fragmentation bad for biodiversity? *Biol. Conserv.*, 230, 179–186.
- 454 Fletcher, R.J., Didham, R.K., Banks-Leite, C., Barlow, J., Ewers, R.M., Rosindell, J., *et al.* (2018). Is  
455 habitat fragmentation good for biodiversity? *Biol. Conserv.*, 226, 9–15.
- 456 Foster, N.L., Foggo, A. & Howell, K.L. (2013). Using Species-Area Relationships to Inform Baseline  
457 Conservation Targets for the Deep North East Atlantic. *PLoS One*, 8, e58941.
- 458 Gilbert, B., Laurance, W.F., Leigh, E.G. & Nascimento, H.E.M. (2006). Can neutral theory predict  
459 the responses of Amazonian tree communities to forest fragmentation? *Am. Nat.*, 168, 304–  
460 317.
- 461 Haddad, N.M., Brudvig, L.A., Clobert, J., Davies, K.F., Gonzalez, A., Holt, R.D., *et al.* (2015). Habitat  
462 fragmentation and its lasting impact on Earth’s ecosystems. *Sci. Adv.*, 1, e1500052–  
463 e1500052.
- 464 Halley, J.M. & Iwasa, Y. (2011). Neutral theory as a predictor of avifaunal extinctions after habitat  
465 loss. *Proc. Natl. Acad. Sci.*, 108, 2316–2321.

- 466 Halley, J.M., Sgardeli, V. & Triantis, K.A. (2014). Extinction debt and the species-area relationship:  
467 A neutral perspective. *Glob. Ecol. Biogeogr.*, 23, 113–123.
- 468 Hansen, M.C., Potapov, P. V, Moore, R., Hancher, M., Turubanova, S.A., Tyukavina, A., *et al.*  
469 (2013). High-resolution global maps of 21st-century forest cover change. *Science*, 342, 850–  
470 3.
- 471 Hanski, I. (2011). Habitat loss, the dynamics of biodiversity, and a perspective on conservation.  
472 *Ambio*, 40, 248–255.
- 473 Hanski, I. & Ovaskainen, O. (2002). Extinction debt at extinction threshold. *Conserv. Biol.*, 16, 666–  
474 673.
- 475 Hanski, I., Zurita, G. a, Bellocq, M.I. & Rybicki, J. (2013). Species-fragmented area relationship.  
476 *Proc. Natl. Acad. Sci.*, 110, 12715–20.
- 477 Hesselbarth, M.H.K., Sciaini, M., With, K.A., Wiegand, K. & Nowosad, J. (2019). landscapemetrics:  
478 an open-source R tool to calculate landscape metrics. *Ecography (Cop.)*, ecog.04617.
- 479 Hubbell, S.P. (2001). The Unified Neutral Theory of Biodiversity and Biogeography. *Monogr.*  
480 *Popul. Biol.*, 17, 375.
- 481 Hubbell, S.P., He, F., Condit, R., Borda-de-Agua, L., Kellner, J. & ter Steege, H. (2008). How many  
482 tree species are there in the Amazon and how many of them will go extinct? *Proc. Natl.*  
483 *Acad. Sci.*, 105, 11498–11504.
- 484 Kalyuzhny, M., Kadmon, R. & Shnerb, N.M. (2015). A neutral theory with environmental

485 stochasticity explains static and dynamic properties of ecological communities. *Ecol. Lett.*,  
486 18, 572–580.

487 Lindenmayer, D.B. & Fischer, J. (2007). Tackling the habitat fragmentation pantheon. *Trends*  
488 *Ecol. Evol.*, 22, 127–132.

489 Lindenmayer, D.B., McCarthy, M. a., Parris, K.M. & Pope, M.L. (2000). Habitat Fragmentation,  
490 Landscape Context, and Mammalian Assemblages in Southeastern Australia. *J. Mammal.*, 81,  
491 787–797.

492 Lindenmayer, D.B., Wood, J., McBurney, L., Blair, D. & Banks, S.C. (2015). Single large versus  
493 several small: The SLOSS debate in the context of bird responses to a variable retention  
494 logging experiment. *For. Ecol. Manage.*, 339, 1–10.

495 May, F., Rosenbaum, B., Schurr, F.M. & Chase, J.M. (2019). The geometry of habitat  
496 fragmentation: Effects of species distribution patterns on extinction risk due to habitat  
497 conversion. *Ecol. Evol.*, 9, 2775–2790.

498 Millenium Ecosystem Assessment. (2005). *Ecosystem and Human Well-Being: Synthesis*. Isl. Press.

499 Miller-Rushing, A.J., Primack, R.B., Devictor, V., Corlett, R.T., Cumming, G.S., Loyola, R., *et al.*  
500 (2019). How does habitat fragmentation affect biodiversity? A controversial question at the  
501 core of conservation biology. *Biol. Conserv.*, 232, 271–273.

502 O’Dwyer, J.P. & Cornell, S.J. (2018). Cross-scale neutral ecology and the maintenance of  
503 biodiversity. *Sci. Rep.*, 8, 1–8.

- 504 Pereira, H.M., Borda-De-Água, L. & Martins, I.S. (2012). Geometry and scale in species-area  
505 relationships. *Nature*, 482, 368–371.
- 506 Rosenzweig, M.L. (1995). *Species diversity in space and time*. Cambridge University Press.
- 507 Rosenzweig, M.L. & Ziv, Y. (1999). The echo pattern of species diversity: pattern and processes.  
508 *Ecography (Cop.)*, 22, 614–628.
- 509 Rosindell, J. & Cornell, S.J. (2007). Species-area relationships from a spatially explicit neutral  
510 model in an infinite landscape. *Ecol. Lett.*, 10, 586–595.
- 511 Rosindell, J. & Cornell, S.J. (2009). Species–area curves, neutral models, and long-distance  
512 dispersal. *Ecology*, 90, 1743–1750.
- 513 Rosindell, J. & Cornell, S.J. (2013). Universal scaling of species-abundance distributions across  
514 multiple scales. *Oikos*, 122, 1101–1111.
- 515 Rosindell, J., Wong, Y. & Etienne, R.S. (2008). A coalescence approach to spatial neutral ecology.  
516 *Ecol. Inform.*, 3, 259–271.
- 517 Rybicki, J. & Hanski, I. (2013). Species-area relationships and extinctions caused by habitat loss  
518 and fragmentation. *Ecol. Lett.*, 16, 27–38.
- 519 Thomas, C.D., Cameron, A., Green, R.E., Bakkenes, M., Beaumont, L.J., Collingham, Y.C., *et al.*  
520 (2004). Extinction risk from climate change. *Nature*, 427, 145–8.
- 521 Thompson, P.L., Rayfield, B. & Gonzalez, A. (2017). Loss of habitat and connectivity erodes species  
522 diversity, ecosystem functioning, and stability in metacommunity networks. *Ecography*

523 (Cop.), 40, 98–108.

524 Tilman, D., May, R.M., Lehman, C.L. & Nowak, M.A. (1994). Habitat destruction and the extinction  
525 debt. *Nature*, 371, 65–66.

526 Tischendorf, L. & Fahrig, L. (2000). On the usage and measurement of landscape connectivity.  
527 *Oikos*, 90, 7–19.

528 Turner, M.G. & Gardner, R.H. (2015). *Landscape Ecology in Theory and Practice*. Springer New  
529 York, New York, NY.

530 Volkov, I., Banavar, J.R., Hubbell, S.P. & Maritan, A. (2003). Neutral theory and relative species  
531 abundance in ecology. *Nature*, 424, 1035–1037.

532 Volkov, I., Banavar, J.R., Hubbell, S.P. & Maritan, A. (2007). Patterns of relative species abundance  
533 in rainforests and coral reefs. *Nature*, 450, 45–49.

534 Wang, X., Blanchet, F.G. & Koper, N. (2014). Measuring habitat fragmentation: An evaluation of  
535 landscape pattern metrics. *Methods Ecol. Evol.*, 5, 634–646.

536 Wilson, M.C., Chen, X.-Y., Corlett, R.T., Didham, R.K., Ding, P., Holt, R.D., *et al.* (2016). Habitat  
537 fragmentation and biodiversity conservation: key findings and future challenges. *Landsc.*  
538 *Ecol.*, 31, 219–227.

539

540

## 541 Figure legends

542 Fig. 1 Three habitat loss scenarios (a–c) and species richness over time averaged across 10  
543 simulations (d–f). The solid and dashed curves represent the result with and without speciation,  
544 respectively; over a 1000 generation timeframe the ability for speciation to offset extinction debt  
545 is negligible (as indeed one would expect in most real situations). The colored areas on the right  
546 represent the equilibrium outcome of species richness within the respective scenario, with  
547 uncertainty obtained from repeated simulations indicated by paler red or blue. For comparison,  
548 an SAR approach for species richness estimation that ignores extinction debt and fragmentation  
549 would predict a species richness of 1020–1400 ( $z$  between 0.1 and 0.3) in all three scenarios  
550 (Appendix 1). For all simulations we used parameters  $A_{\max} = 500^2$ ,  $h = 20\%$ ,  $\nu = 0.0001$ ,  
551  $\sigma = 16$ .

552 Fig. 2 The unscaled (a) and rescaled (b) SARs from our simulations (obtained by dividing the  
553 effective area axis and the species richness axis, by the squared effective connectivity,  $c_e^2$ ). The re-  
554 scaling collapses the parameter space to its equivalent in a contiguous landscape, and the  
555 resulting points fall approximately on a single curve. MPEs are 4.91% (contiguous), 9.09%  
556 (clustered), 4.17% (random) and 8.08% (real). Parameters used were all combinations of  $\sigma$  in  
557  $\{8, 16, 32\}$ ,  $A_{\max}$  in  $\{50^2, 500^2, 5000^2\}$ , and  $h$  in  $\{10, 20, 40\}$  for each landscape type, with  
558  $\nu = 0.0001$ .

559 Fig. 3 The equilibrium percentage of species richness remaining after habitat loss, including the  
560 uncertainty range obtained from differences in fragmentation, as a function of total area,  $A_{\max}$ .  
561 Dark red indicates best-case immediate loss after habitat loss. Paler red indicates worst-case

562 immediate loss and thus shows the uncertainty around immediate loss based on habitat  
563 configuration. Dark blue areas show the remaining species at equilibrium in the longer term, after  
564 extinction debt has been paid. Paler blue shows species that remain in the longer term in the  
565 best-case scenario depending on the habitat configuration. Pale grey represents the definite  
566 extinction debt as the gap between the worst-case immediate loss and best-case long-term loss  
567 results. The actual values of richness after immediate loss and in the long-term will occur in the  
568 pale red and pale blue pale colored areas respectively, and depend upon the structure of the  
569 fragmented landscape (see Fig. 4 for an example of equilibrium richness corresponding to the  
570 center panel). Here,  $\nu = 0.0001$ .

571 Fig. 4 Percentage of species richness remaining in the long-term as a function of total habitat  
572 area. Each point represents the mean value of species richness (vertical axis) from simulations on  
573 one landscape of area  $A_{\max}$  (horizontal axis) and effective connectivity  $c_e$  (colors). For all points,  
574 habitat cover is  $h = 20\%$  and the dispersal parameter is  $\sigma = 16$ , corresponding to the central  
575 panel from Fig. 3. Theoretical bounds our formulas are given by the dashed and dotted lines for  
576 the upper and lower bounds, respectively. The region (Appendix 3) between these bounds  
577 corresponds directly to the pale blue region in the central panel of Fig. 3. Real landscapes occupy  
578 a subset of parameter space, indicated by the grey shaded region. The three triangles represent  
579 the results from simulations performed on three landscapes of equal effective area ( $A_e = hA_{\max}$ )  
580 indicated on the right.

581 Fig. 5 Summary of expected species richness outcomes at different spatiotemporal scales and  
582 under different levels of habitat loss and fragmentation. This figure conveys the qualitative  
583 patterns that hold across parameter space. Here,  $\sigma = 16$ ,  $\nu = 0.0001$ ,  $A_{\max} \in \{10^4, 10^6, 10^8\}$

584 (for local, intermediate and regional spatial scale, respectively) and  $h \in \{0.8, 0.4, 0.2\}$  (for low,  
585 medium and high habitat loss, respectively). The extremes of habitat connectivity  $c_e$  at each  
586 spatial scale were determined using our full range of real landscapes to determine the lower  
587 bound, and using random landscapes to determine the upper bound. Warmer colors indicate  
588 fewer species remaining (more severe species loss).

589 Fig. 6 Different methods of estimating species richness in a fragmented landscape. The approach  
590 of Chisholm *et al.* (2018) gives bounds for the species richness immediately following habitat loss  
591 (red area). Our approach gives bounds for the long-term species richness (blue area). The  
592 traditional power-law approach provides a phenomenological estimate of species richness  
593 without reference to temporal scale (brown area). Predictions for tree species losses in five 10  
594 km<sup>2</sup> areas of the Amazon are shown using the effective connectivity metric with  $\sigma = 8.5$   
595 (approximately 40.2 m) and  $\nu = 6 \times 10^{-6}$  (Condit *et al.* 2002). The approach for predicting the  
596 tree species losses is outlined in Appendix 7. Abbreviations for locations: Elc, El Cayman,  
597 Colombia; Rio, Rio Branco, Brazil; Ari, Ariquemes, Brazil; Atl, Altamira, Brazil; Mar, Maraba, Brazil.



Figure 1.

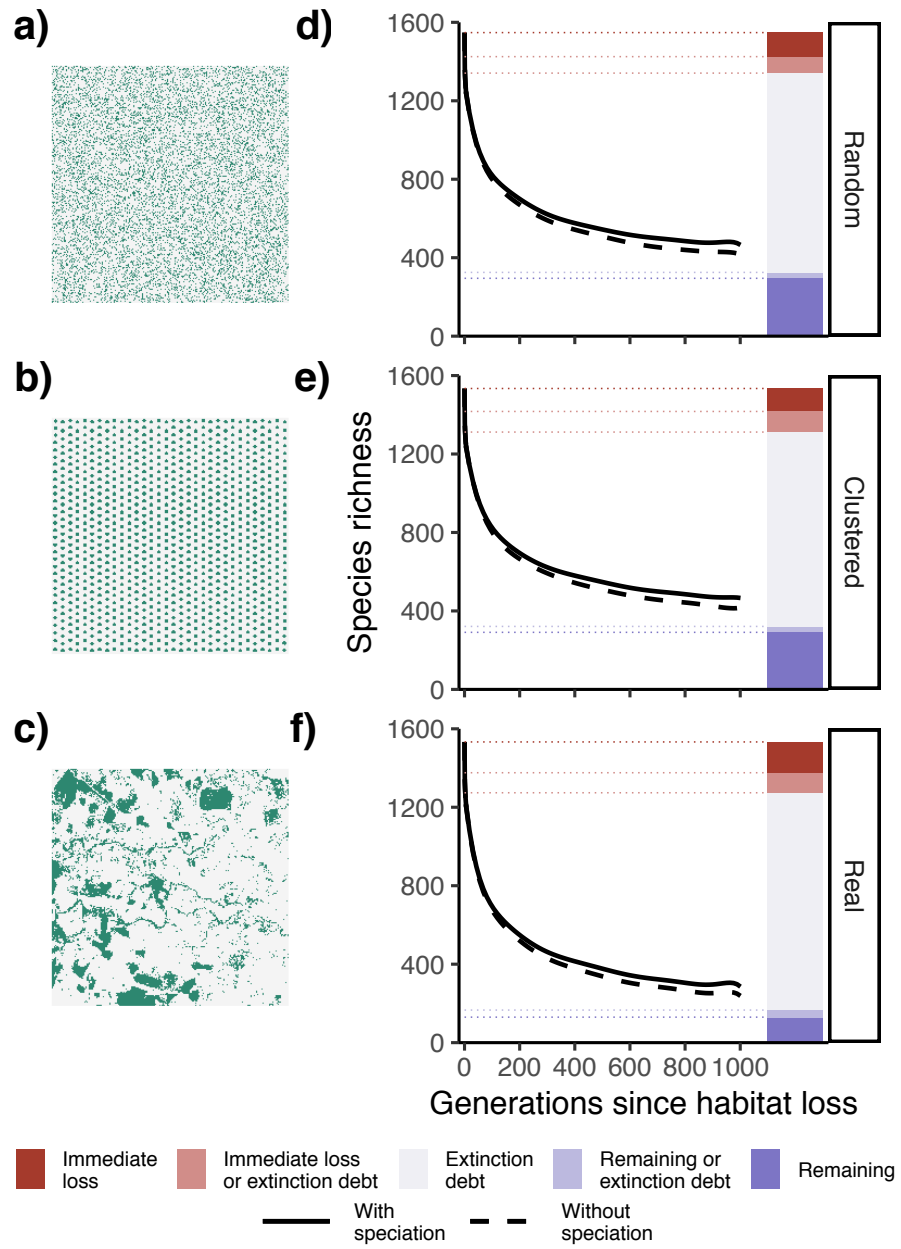


Figure 2.

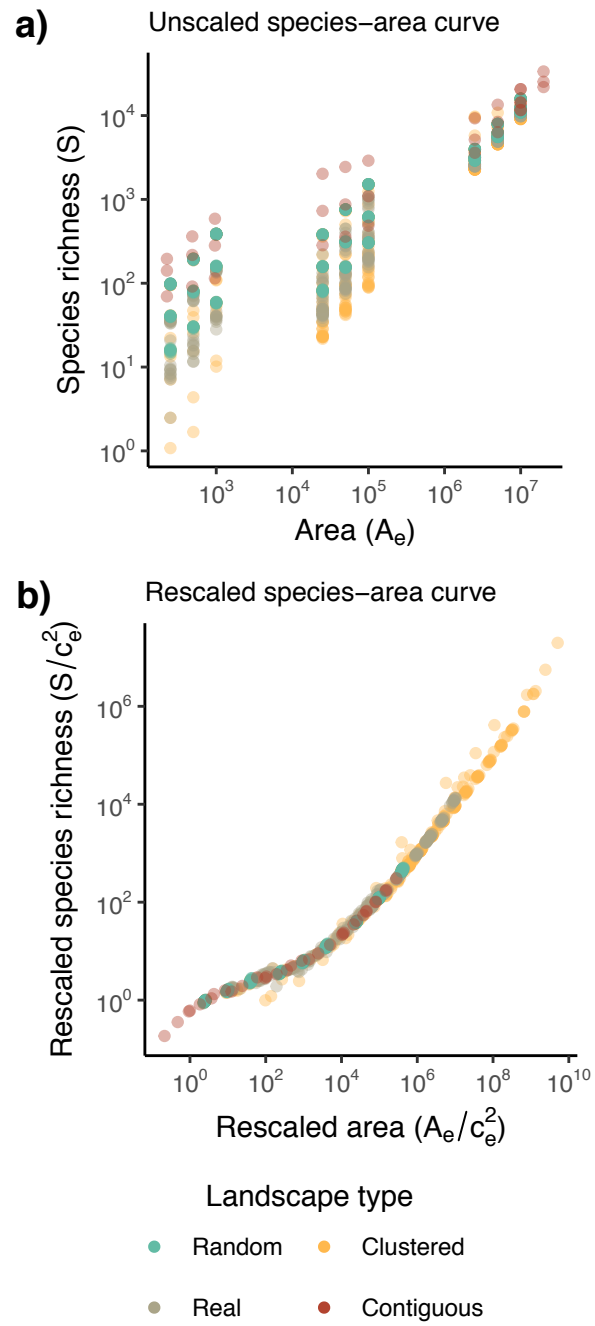


Figure 3.

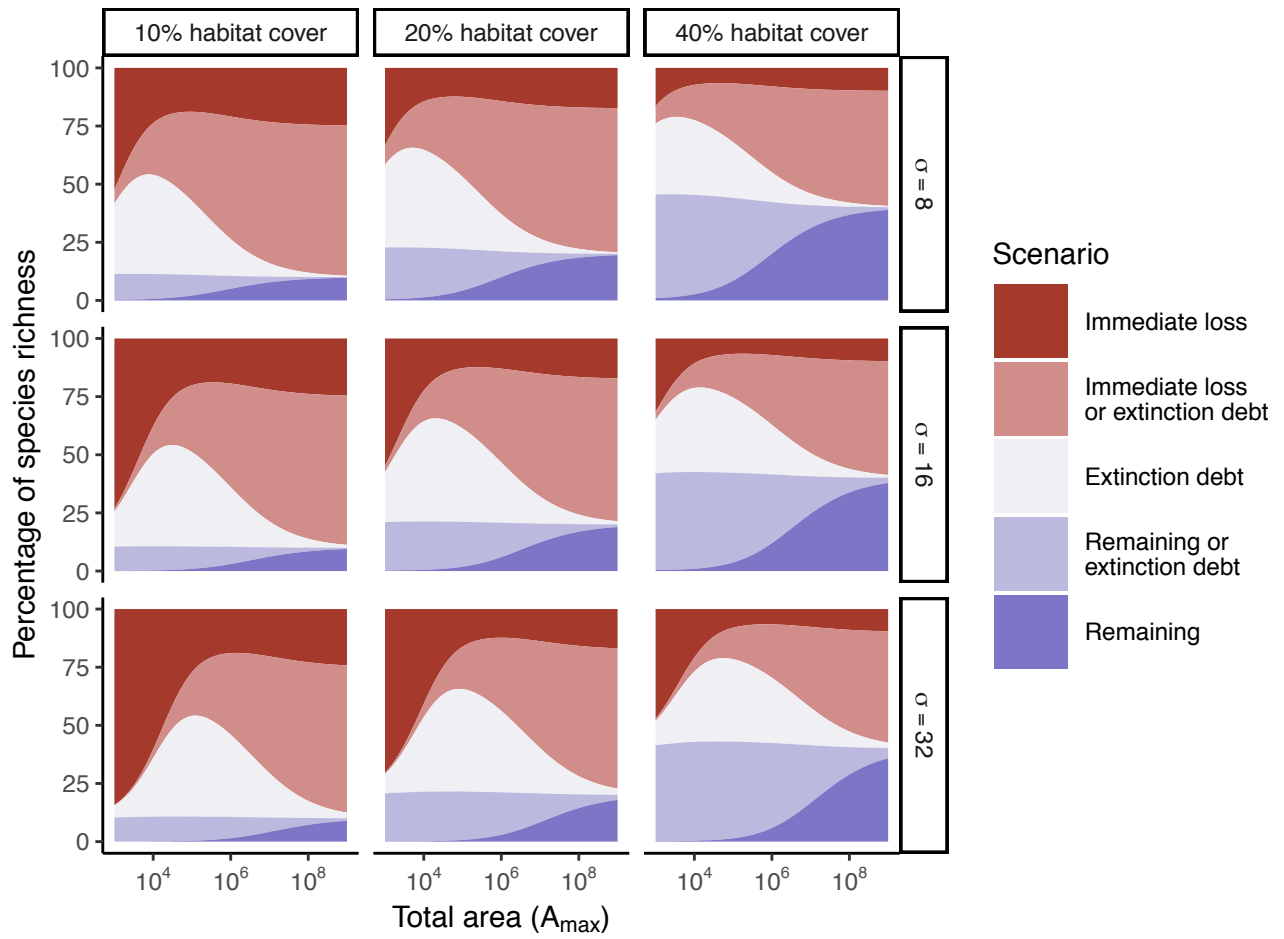


Figure 4.

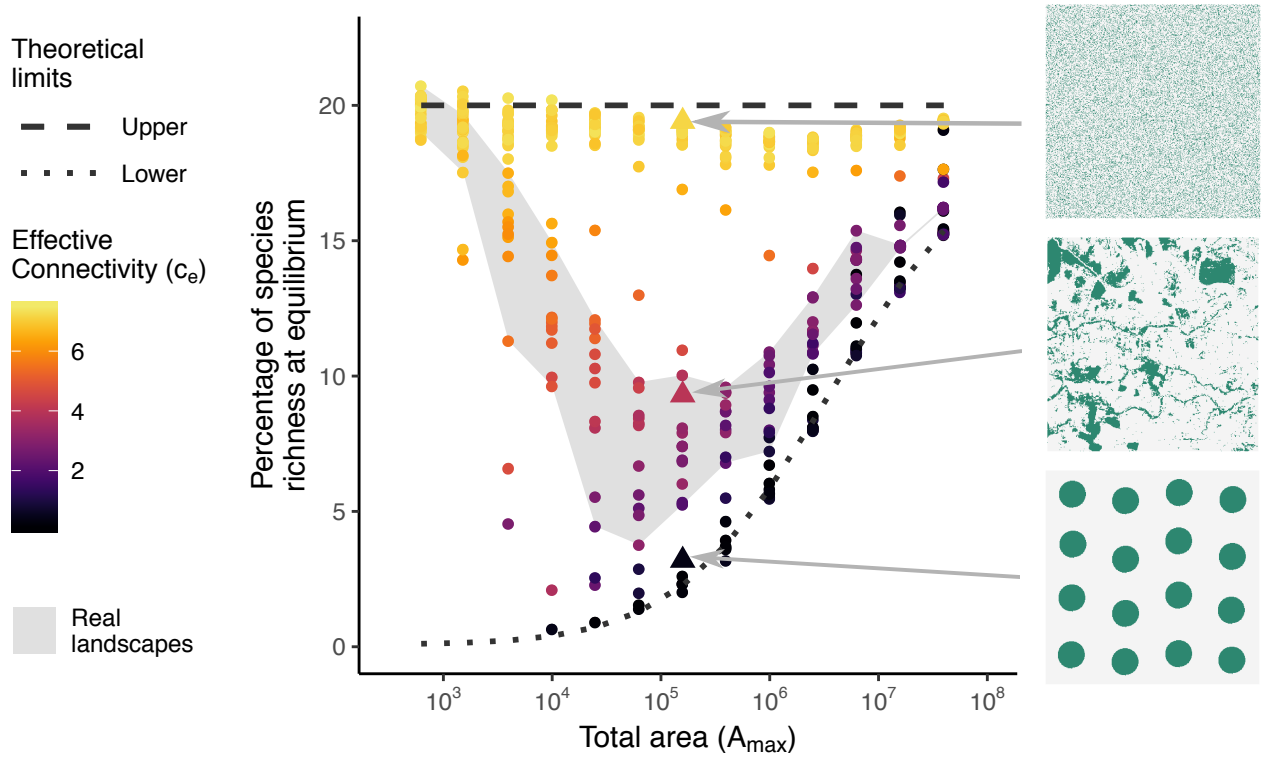


Figure 5.

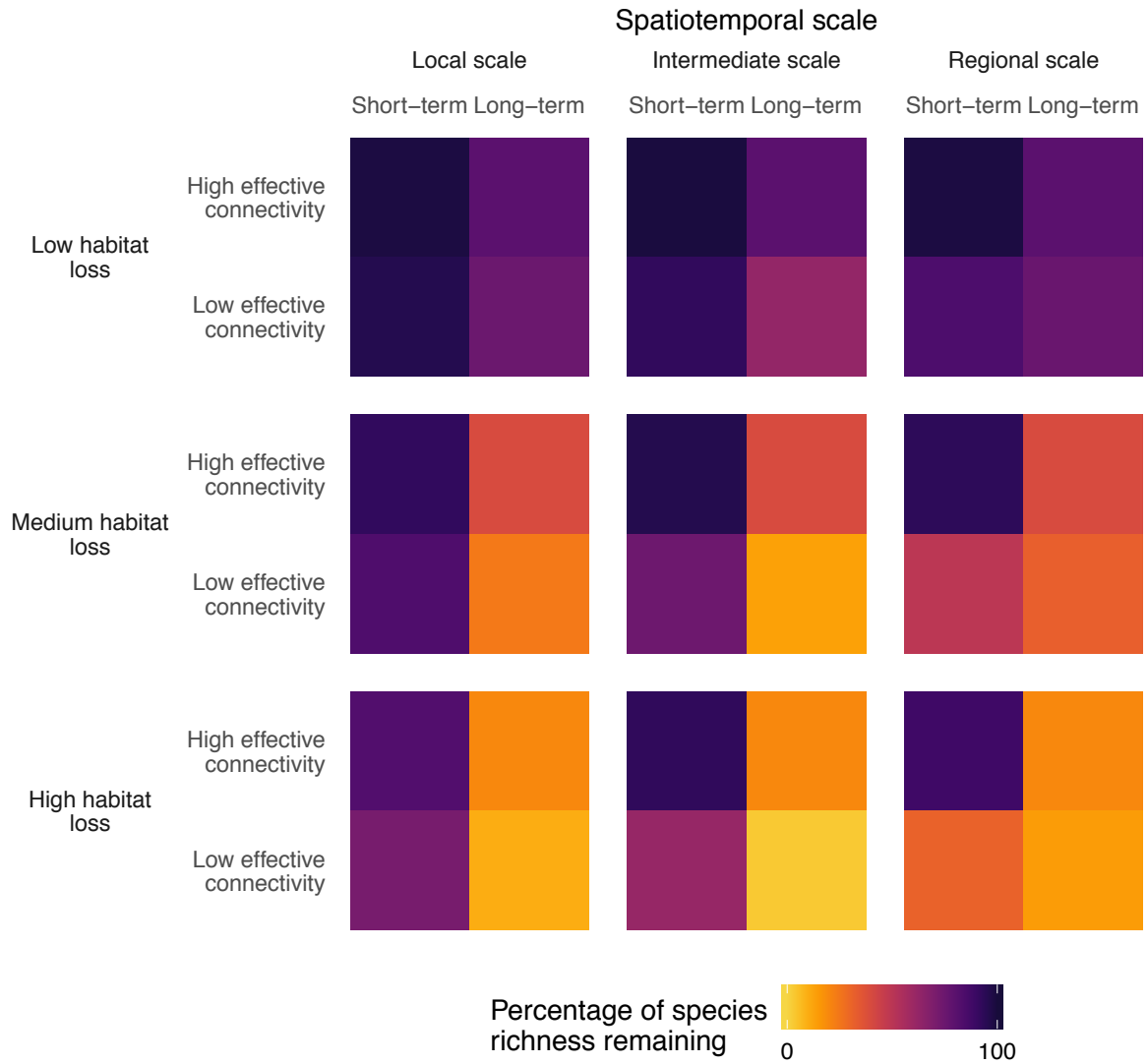


Figure 6.

